ACS OMEGA

http://pubs.acs.org/journal/acsodf

Article

Imidazole Acceptor for Both Vacuum-Processable and Solution-Processable Efficient Blue Thermally Activated Delayed Fluorescence

Yu Kusakabe, Yoshimasa Wada, Tomoya Misono, Katsuaki Suzuki, Katsuyuki Shizu, and Hironori Kaji*

Cite This: *ACS Omega* 2022, 7, 16740−16745

Read Online

ACCESS | Metrics & More | Article Recommendations | Supporting Information

ABSTRACT: The members of the imidazole family have been widely used for electron transporting, host, conventional fluorescent, and phosphorescent materials. Although the imidazole core also has great potential as an acceptor segment of deep-blue thermally activated delayed fluorescence (TADF) owing to its high triplet energy, the emission color of imidazole-based TADF organic light-emitting diodes (OLEDs) has so far been limited to blue to green. In this work, four acridan-imidazole systems are theoretically designed aiming for deep- or pure-blue emitters. All four emitters exhibit deep-blue to blue emission owing to the high energy levels of the lowest excited singlet states, exhibiting *y* coordinates of Commission Internationale de l'Eclairage coordinates between 0.06 and 0.26. The molecule composed of a trifluoromethyl-substituted benzimidazole acceptor in combination with a tetramethyl-9,10-dihydroacridine donor (named MAc-FBI) achieves a high maximum external quantum efficiency (EQE_{MAX}) of 13.7% in its application to vacuum-processed OLEDs. The emitter has high solubility even in ecofriendly nonhalogenated solvents, which motivates us to fabricate solution-processed MAc-FBI-based OLEDs, resulting in an even higher EQE_{MAX} of 16.1%.

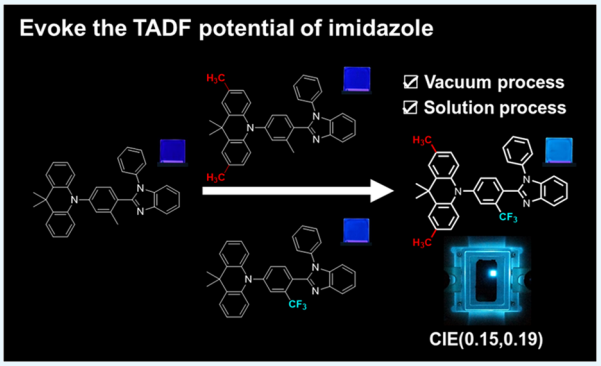

1. INTRODUCTION

To boost the performance of the organic light-emitting diodes (OLEDs), thermally activated delayed fluorescence (TADF) materials have been widely adopted to OLEDs as emitters.[1−8] This is because TADF materials can convert all singlet and triplet excitons into light through reverse intersystem crossing (RISC) owing to the small energy difference (ΔE_{ST}) between the lowest excited singlet state (S_1) and the lowest triplet state (T_1). To achieve small ΔE_{ST}, the separation between the highest occupied molecular orbital (HOMO) and the lowest unoccupied molecular orbital (LUMO) is valid. Therefore, the combination of electron donor and acceptor fragments has been incorporated into TADF molecular design. Imidazole is a widely used molecular fragment for OLED materials such as electron transporting materials, host materials, and emitter materials. This is because of their good tunability of photophysical and electrical properties derived from both an electron-donating and an electron-accepting imidazole core, as has been reviewed in ref 9. Thus, imidazole is one of the good candidates for the molecular fragments of TADF materials. So far, five reports have been found for TADF emitters that possess an imidazole core in their application to OLEDs.[10−14] Wang and co-workers reported two phenanthroimidazole-based green TADF emitters, named PPZTPI and PPZPPI.[10] For benzimidazole (BI)-based TADF emitters, Adachi and co-workers reported a green emitter named DHPZ-2BI,[11] and Zysman-Colman and co-workers also reported four green emitters.[12] Kido and co-workers reported a series of BI-based emitters and one of which was named PXZ-BIP exhibited sky-blue emission in Commission Internationale de l'Eclairage (CIE) coordinates (*x*, *y*) of (0.22, 0.42).[13] Lu and co-workers reported dicyanoimidazole-based emitters named imM-SPAC and imM-DMAC that showed blue emissions with CIE coordinates of (0.17, 0.18) and (0.16, 0.19), respectively.[14]

Considering the high LUMO energy level and high T_1 energy of the imidazole core, we can expect efficient deep- or pure-blue TADF materials by appropriate molecular modification. In this work, we investigate four donor−acceptor-type emitters (Figure 1) using BI-derivatives as acceptors in combination with 9,10-dihydro-9,9-dimethylacridine (Ac) electron-donating derivatives. All emitters exhibited blue emission ranging from deep-blue to blue in their doped films. Among the four, MAc-FBI (Figure 1), which has the combination of a 2,7,9,9-tetramethyl-9,10-dihydroacridine donor (MAc) and 1-phenyl-2-(2-(trifluoromethyl)phenyl)-

Received: March 4, 2022
Accepted: April 20, 2022
Published: May 4, 2022

https://doi.org/10.1021/acsomega.2c01308
ACS Omega 2022, 7, 16740−16745

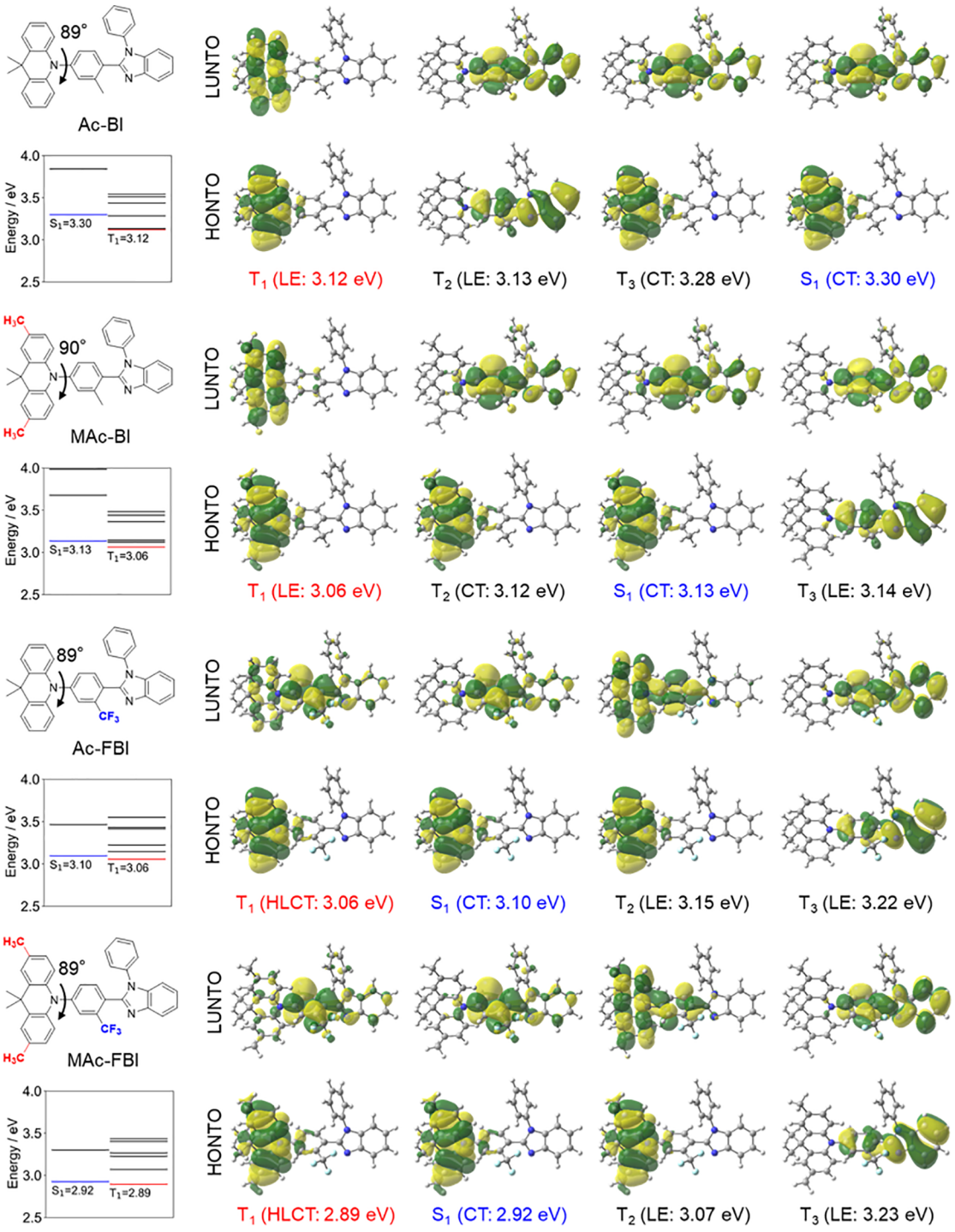

Figure 1. Molecular structures, energy levels of excited states, and natural transition orbitals of respective excited states for Ac-BI, MAC-BI, Ac-FBI, and MAc-FBI.

Table 1. TD-DFT Calculated and Experimental Data of Ac-BI, MAc-BI, Ac-FBI, and MAc-FBI

emitter	HOMO [eV]	LUMO [eV]	E_g [eV]	S_1 [eV]	T_1 [eV]	T_2 [eV]	T_3 [eV]	ΔE_{ST} [eV]
Ac-BI	−5.46	−1.38	4.09	3.30[a]/3.44[b]	3.12[a]/3.00[b]	3.13	3.28	0.18[a]/0.44[b]
MAc-BI	−5.25	−1.34	3.90	3.13[a]/3.28[b]	3.06[a]/2.95[b]	3.12	3.14	0.07[a]/0.33[b]
Ac-FBI	−5.61	−1.66	3.95	3.10[a]/3.19[b]	3.06[a]/2.92[b]	3.15	3.22	0.04[a]/0.27[b]
MAc-FBI	−5.39	−1.63	3.76	2.92[a]/3.08[b]	2.89[a]/2.94[b]	3.07	3.23	0.03[a]/0.14[b]

[a]Calculated values. [b]Experimental values.

1H-benzo[*d*]imidazole (FBI), exhibits efficient TADF and achieves a EQE_{MAX} = 13.7% with blue emission of CIE (0.15, 0.19) in its application to vacuum-processed OLEDs. In addition, MAc-FBI is found to be highly soluble in non-

https://doi.org/10.1021/acsomega.2c01308
ACS Omega 2022, 7, 16740−16745

halogenated solvents, which motivated us to fabricate solution-processed OLEDs as well. The EQE_{MAX} reached 16.1% with blue emission of CIE (0.17, 0.24). Both vacuum- and solution-processable features of MAc-FBI make it an attractive TADF emitter for OLEDs.

2. RESULTS AND DISCUSSION

2.1. Molecular Design. The four molecules, Ac-BI, MAc-BI, Ac-FBI, and MAc-FBI, were designed using Ac as an electron donor core and BI as an acceptor core (Figure 1). Here, calculations were conducted using Gaussian 16,[15] and the results are summarized in Table 1, Figures 1, and S5. Molecular geometries were optimized using density functional theory (DFT) at the ground state (S_0) with the PBE0/6-311++G(d,p) level of theory considering toluene solvent polarity effects using the polarizable continuum model (PCM). Calculations for the excited states were also conducted using time-dependent DFT (TD-DFT) with the same basis set and the PCM condition using the S_0 optimized structure. Torsion angles between donors and acceptors were large (89−90°), which resulted in adequate separation of the HOMO and LUMO distributed on the donor and acceptor units, respectively (Figure S1). The HOMO energy level of MAc-BI and MAc-FBI was higher than that of Ac-BI and Ac-FBI because of CH_3 substitution in Ac. Also, owing to the CF_3 substitution in BI, the LUMO energy level of Ac-FBI and MAc-FBI was lower than that of Ac-BI and MAc-BI, as we designed. The calculated ΔE_{ST} values for the S_0 structures were within 0.2 eV for the four molecules; Ac-BI (0.18 eV), MAc-BI (0.07 eV), Ac-FBI (0.04 eV), and MAc-FBI (0.03 eV), as shown in Table 1.

The origin of the difference in ΔE_{ST} between the four emitters was investigated by natural transition orbital (NTO) analysis. The highest occupied NTO (HONTO) and lowest unoccupied NTO (LUNTO) are provided in Figure 1. For all of the molecules, the HONTOs and LUNTOs of S_1 were distributed on the donors and acceptors, respectively, which is characteristic of charge transfer (CT) states. The energy gaps between the CT-type S_1 and the lowest CT-type or CT-dominant hybridized local CT (HLCT)-type triplet (T_3 for Ac-BI, T_2 for MAc-BI, T_1 for Ac-FBI, and T_1 for MAc-FBI) were small. In contrast to HLCT T_1 states of Ac-FBI and MAc-FBI, the T_1s of Ac-BI and MAc-BI were locally excited type triplet (^{3}LE) states. Owing to the lower-lying ^{3}LE in energy, these two molecules, especially Ac-BI, exhibited relatively large ΔE_{ST}s. From HOMO energy levels, LUMO energy levels, and NTO analysis, thanks to CH_3 and CF_3 substitution in Ac and BI, respectively, appropriate CT-type S_1 energies were expected for the small ΔE_{ST} in MAc-BI, Ac-FBI, and especially MAc-FBI.

2.2. Photophysical Property of Emitters. The four molecules were synthesized and purified by train sublimation for further photophysical measurements (see the Supporting Information for details). Figure 2a exhibits their UV−vis absorption and photoluminescence (PL) spectra in a 10^{-5} M toluene solution. A broad and weak absorption shoulder with an absorption coefficient ε of ∼2000 M^{-1} cm^{-1} was observed at approximately 350−400 nm. The absorption energies decreased in the order of Ac-BI, MAc-BI, Ac-FBI, and MAc-FBI. All of the molecules exhibited blue emission. Emission spectra at room temperature were red-shifted in the order of a maximum emission wavelength (λ_{MAX}) of 422 nm (Ac-BI), 442 nm (MAc-BI), 463 nm (Ac-FBI), and 485 nm (MAc-FBI).

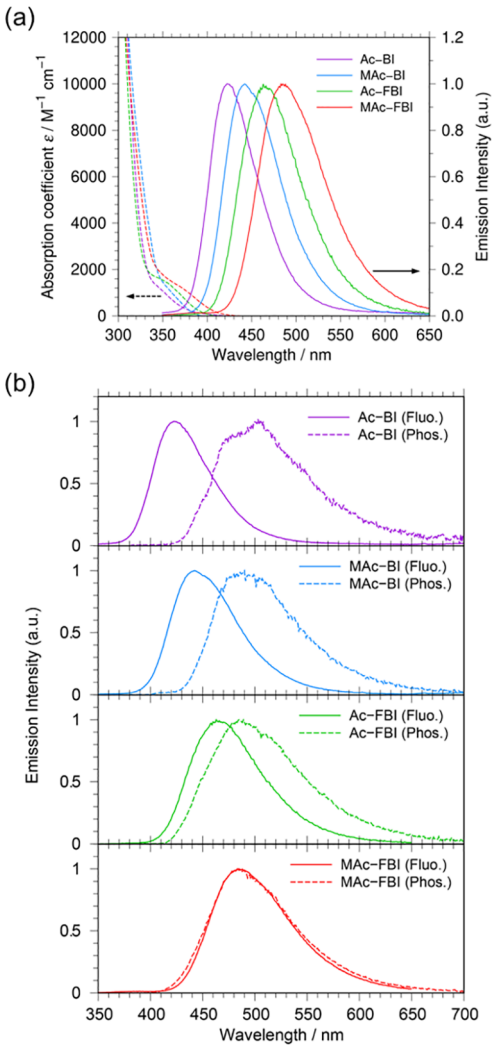

Figure 2. (a) UV−vis absorption and PL spectra at room temperature and (b) fluorescence (Fluo.) and phosphorescence (Phos.) spectra of Ac-BI, MAc-BI, Ac-FBI, and MAc-FBI at 77 K. Fluorescence and phosphorescence spectra were integrated into the time range of 10−50 μs and 300−600 ms, respectively, after the light pulse excitation.

Figure 2b shows the fluorescence and phosphorescence spectra at 77 K. Fluorescence and phosphorescence spectra were integrated for a time range of 10−50 μs and 300−600 ms, respectively, after the light pulse excitation. The ΔE_{ST}s were determined from the onsets of the fluorescence and phosphorescence spectra: Ac-BI (0.44 eV), MAc-BI (0.33 eV), Ac-FBI (0.27 eV), and MAc-FBI (0.14 eV). Experimental data of S_1, T_1, and ΔE_{ST} in a 10^{-5} M toluene solution are also summarized in Table 1. The experimental ΔE_{ST}s (0.14−0.44 eV) were greater than the calculated ones (0.03−0.18 eV). Thus, we reevaluated the ΔE_{ST}s of the four emitters by high-level two kinds of calculations. One was the second-order algebraic diagrammatic construction (ADC(2)) method and the other was the spin-component scaling second-order approximate coupled-cluster (SCS-CC2). Here, ADC(2) and SCS-CC2 calculations were carried out using the TURBOMOLE software package.[16,17] The calculated S_1, T_1, ΔE_{ST}, and experimental ΔE_{ST} are summarized in Table S1. Compared with the calculated ΔE_{ST}s of ADC(2), those of SCS-CC2 were in good agreement with the experimental ΔE_{ST}s for all emitters in this work.

https://doi.org/10.1021/acsomega.2c01308
ACS Omega 2022, 7, 16740−16745

Table 2. Photophysical Properties of Ac-BI, MAc-BI, Ac-FBI, and MAc-FBI in a DPEPO and CzSi Host Spin-coated Film at an Excitation Wavelength of 300 nm[a]

host	emitter	λ_{MAX} [nm]	CIE[c] (x, y)	Φ_{PL}[c] [%]	delayed fluorescence[d]
DPEPO	Ac-BI	416[b]/419[c]	(0.16, 0.07)	20.7 ± 0.1	
	MAc-BI	440[b]/440[c]	(0.16, 0.12)	31.6 ± 0.7	detected
	Ac-FBI	462[b]/451[c]	(0.16, 0.15)	56.2 ± 0.1	detected
	MAc-FBI	482[b]/473[c]	(0.18, 0.26)	64.2 ± 0.4	detected
CzSi	Ac-BI	410[b]/412[c]	(0.17, 0.06)	18.9 ± 0.1	
	MAc-BI	426[b]/429[c]	(0.16, 0.08)	20.3 ± 0.0	
	Ac-FBI	439[b]/446[c]	(0.16, 0.11)	29.2 ± 0.1	detected
	MAc-FBI	468[b]/465[c]	(0.16, 0.20)	46.9 ± 0.1	detected

[a]Φ_{PL}s were determined to be average value ± error (95% confidence interval). [b]Measured under an air condition. [c]N_2 flow. [d]He atmosphere.

The photophysical performances of the four emitters in the solid films were investigated using spin-coated amorphous films prepared from chloroform solution. Emitters were doped at a concentration of 10 wt % in a host matrix, bis[2-(diphenylphosphino)phenyl]ether oxide (DPEPO)[18] or 9-(4-tert-butylphenyl)-3,6-bis(triphenylsilyl)-9H-carbazole (CzSi),[19] which are typically used for blue TADF emitters.[20] As summarized in Table 2, Ac-BI exhibited the deepest blue emission among the four molecules, with CIE (0.16, 0.07) in DPEPO and (0.17, 0.06) in CzSi. Even the most red-shifted emitter, MAc-FBI, still showed blue emission of CIE (0.18, 0.26) in DPEPO and CIE (0.16, 0.20) in CzSi (also see Figure 3). To obtain the ΔE_{ST}s of these emitters in the films, we

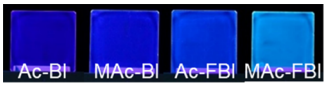

Figure 3. Photographs of 10 wt % emitter: CzSi spin-coated film. From left to right, Ac-BI, MAc-BI, Ac-FBI, and MAc-FBI.

collected fluorescence and phosphorescence spectra at 77 K using DPEPO as the host (Figure S6). The S_1, T_1, and ΔE_{ST} values of all emitters in toluene solutions and in DPEPO films are summarized in Table S3.

Photoluminescence quantum yields (PLQYs) and transient PL decay curves are shown in Table 2 (also see Figure S7). Ac-BI exhibited a low PLQY of ∼20% and did not show clear delayed fluorescence in both DPEPO and CzSi. MAc-BI exhibited almost the same PLQY of 20%, and no clear delayed emission was observed in CzSi, while a higher PLQY of 30% was obtained, and delayed fluorescence was observed in DPEPO. Ac-FBI displayed delayed fluorescence in both CzSi and DPEPO. The PLQY was still low (29%) in CzSi, while an improved PLQY of 56% was obtained in DPEPO. MAc-FBI exhibited the best performance: clear delayed fluorescence in both hosts and relatively high PLQYs of 47% in CzSi and 56% in DPEPO. From temperature-dependent transient PL measurement for MAc-BI, Ac-FBI, and MAc-FBI doped in DPEPO films, the delayed fluorescence was confirmed to be thermal activated (see Figure S8). These TADF characteristics and PLQYs are well explained by the above-mentioned experimental ΔE_{ST}s of the four emitters.

Table 3 shows the prompt lifetime (τ_p) and delayed lifetime (τ_d) of the materials' detected delayed fluorescence, determined from the fitting of the PL decay curves with double exponential functions. The τ_ds were relatively long (20−90 μs). To obtain deeper insight into the long τ_d, we determined rate constants for radiative (k_r), nonradiative (k_{nr}), ISC (k_{ISC}), and RISC (k_{RISC}) transitions based on the previously reported method[21] (Table 3). MAc-BI, Ac-FBI, and MAc-FBI exhibited k_{RISC} of 10^{4-5} s^{-1}, leading to delayed PL lifetimes on the order of 20−90 μs. Owing to the greater k_{ISC} compared to k_r and k_{nr}, photoexcited singlet excitons tend to be converted into triplet excitons. Then, some excitons are assumed to decay nonradiatively, resulting in moderate PLQYs, as shown in Table 2.

2.3. Organic Light-Emitting Diodes. We fabricated both vacuum- and solution-processed OLEDs using the MAc-FBI emitter doped in the CzSi host to achieve efficient blue emission. As shown in Figure S9a, the device structure of the vacuum-processed OLED was indium−tin−oxide (ITO) (50 nm)/4,4′-cyclohexylidenebis[N,N-bis(4-methylphenyl)-benzenamine] (TAPC) (60 nm)/1,3-bis(9,9-dimethylacridin-10(9H)-yl)benzene (mAP) (10 nm)/10 vol % MAc-FBI:CzSi (20 nm)/2,8-bis(diphenylphosphoryl)dibenzo[b,d]furan (PPF) (10 nm)/1,3-bis[3,5-di(pyridin-3-yl)phenyl]benzene (BmPyPhB) (30 nm)/lithium quinolin-8-olate (Liq) (1 nm)/Al (80 nm). As shown in Figure 4 and Table S4, the OLED exhibited blue emission with CIE (0.15, 0.19) and EQE_{MAX} was 13.7%. We also investigated the solution-processed OLEDs with a device structure of ITO (50 nm)/poly(3,4-ethylenedioxythiophene) polystyrene sulfonate (PE-

Table 3. Values of τ_p, τ_d, Φ_p, Φ_d, k_r, k_{nr}, k_{ISC}, and k_{RISC} of 10 wt % *Emitter*-Doped Films, Where Emitters Were MAc-BI, Ac-FBI, and MAc-FBI[ab]

host	emitter	τ_p [ns]	τ_d [μs]	Φ_p [%]	Φ_d [%]	k_r ($S_1 \rightarrow S_0$) [10^6 s^{-1}]	k_{nr} ($T_1 \rightarrow S_0$) [10^3 s^{-1}]	k_{ISC} [10^7 s^{-1}]	k_{RISC} [10^4 s^{-1}]
DPEPO	MAc-BI	5.7	22.2	8.8	22.8	15.3	6.2	15.9	2.4
	Ac-FBI	12.8	69.7	10.9	45.3	8.6	7.1	7.0	6.7
	MAc-FBI	22.8	33.3	13.2	51.0	5.8	12.4	3.8	13.3
CzSi	Ac-FBI	10.8	86.2	14.1	15.1	13.1	9.6	8.0	1.5
	MAc-FBI	14.9	66.6	8.9	38.0	6.0	8.8	6.1	7.0

[a]Φ_p, Φ_d, k_r, and k_{nr} are the Φ_{PL} of the prompt component, Φ_{PL} of the delayed component, the rate constant of radiative decay from S_1, and nonradiative decay from T_1, respectively. [b]Rate constants were deduced based on the previously reported method.[21]

https://doi.org/10.1021/acsomega.2c01308
ACS Omega 2022, 7, 16740−16745

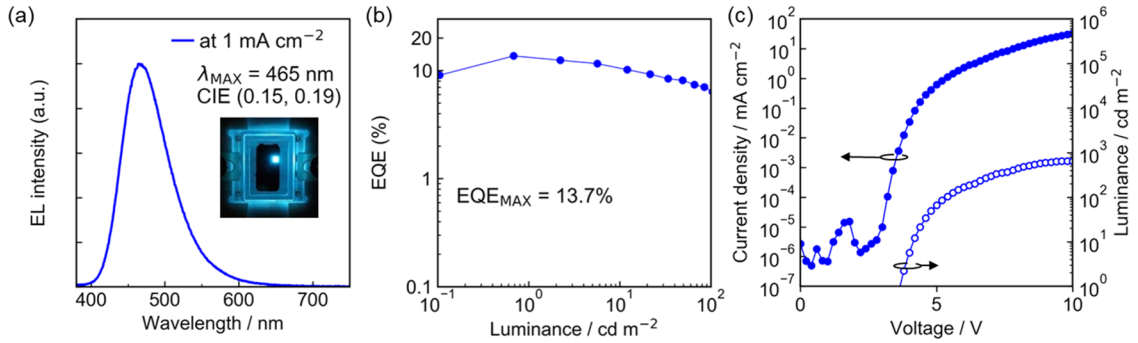

Figure 4. Performance of vacuum-processed OLEDs using 10 vol % MAc-FBI:CzSi as the emitting layer. (a) Electroluminescence (EL) spectrum at 1 mA cm^{-2}, which corresponds to 100 cd m^{-2} and (b) EQE−luminance curve and (c) current density−voltage−luminance characteristics.

DOT:PSS) (35 nm)/poly(9-vinylcarbazole) (PVK) (10 nm)/10 wt % MAc-FBI:CzSi (20 nm)/PPF (5 nm)/1,3,5-tris(1-phenyl-1H-benzo[*d*]imidazol-2-yl)benzene (TPBi) (50 nm)/Liq (1 nm)/Al (80 nm) (see Figure S9b). Here, the PEDOT:PSS, PVK, and 10 wt % MAc-FBI:CzSi layers were fabricated by spin-coating and the following layers were vacuum deposited. We prepared an emitter layer solution using toluene because MAc-FBI is highly soluble in toluene with a solubility of more than 10 mg mL^{-1}. The high solubility in such a nonhalogenated solvent is a great advantage for the fabrication of solution-processed multilayer OLEDs[22] and the halogen-free process is attractive for environmentally friendly OLED production.[23,24] Compared with the vacuum-processed OLED, the solution-processed OLED exhibited a higher EQE_{MAX} of 16.1% with a slightly red-shifted blue emission with CIE (0.17, 0.24) (Figure S3 and Table S4). These good device performances of MAc-FBI in both vacuum-processed and solution-processed OLEDs demonstrate that the imidazole core is a promising candidate for designing blue TADF.

3. CONCLUSIONS

We report four emitters, Ac-BI, MAc-BI, Ac-FBI, and MAc-FBI, using an acridan-benzimidazole donor−acceptor system. From the theoretical calculations, the four emitters exhibited a sufficiently high S_1 energy to show blue emission, owing to the wide HOMO−LUMO gap, which results from the combination of the deep HOMO of the Ac core and the shallow LUMO of the BI core. In addition to the high S_1, MAc-FBI exhibited the smallest ΔE_{ST} among the four emitters, owing to the good combination of MAc and FBI, which were modified from Ac and BI, respectively. Experimentally, all four molecules exhibited blue emissions. MAc-BI, Ac-FBI, and MAc-FBI exhibited the typical photophysical feature of TADF. Vacuum-processed OLEDs using an MAc-FBI emitter exhibited an EQE_{MAX} of 13.7% with blue emission of CIE (0.15, 0.19). Furthermore, MAc-FBI was found to be highly soluble in an environment-friendly nonhalogenated solvent. Solution-processed OLEDs using MAc-FBI as an emitter were fabricated and exhibited a higher EQE_{MAX} of 16.1% with blue emission of CIE (0.17, 0.24). Both the vacuum- and solution-processability of MAc-FBI demonstrated in this work reveals part of the potential of an imidazole core for the design of deep- or pure-blue TADF materials.

ASSOCIATED CONTENT

Supporting Information

The Supporting Information is available free of charge at https://pubs.acs.org/doi/10.1021/acsomega.2c01308.

Experimental procedure including synthesis, photophysical measurements, preparation of the samples, and device characterization and additional scheme or figure or table of synthesis, theoretical investigation, photophysical properties, and device performances (PDF)

AUTHOR INFORMATION

Corresponding Author

Hironori Kaji − *Institute for Chemical Research, Kyoto University, Uji, Kyoto 611-0011, Japan;* orcid.org/0000-0002-5111-3852; Email: kaji@scl.kyoto-u.ac.jp

Authors

Yu Kusakabe − *Institute for Chemical Research, Kyoto University, Uji, Kyoto 611-0011, Japan*

Yoshimasa Wada − *Institute for Chemical Research, Kyoto University, Uji, Kyoto 611-0011, Japan;* orcid.org/0000-0001-6139-8794

Tomoya Misono − *Institute for Chemical Research, Kyoto University, Uji, Kyoto 611-0011, Japan*

Katsuaki Suzuki − *Institute for Chemical Research, Kyoto University, Uji, Kyoto 611-0011, Japan*

Katsuyuki Shizu − *Institute for Chemical Research, Kyoto University, Uji, Kyoto 611-0011, Japan;* orcid.org/0000-0002-1835-0418

Complete contact information is available at: https://pubs.acs.org/10.1021/acsomega.2c01308

Author Contributions

Y.K., Y.W., T.M., and K.S. conducted quantum chemical calculations; T.M. and K.S. contributed to the synthesis of the materials; T.M. performed material characterization; Y.K. contributed to the device structure; Y.K., Y.W., and T.M. contributed to device fabrication; and H.K. planned and supervised the study. All authors wrote the manuscript and approved the final version of the manuscript.

Notes

The authors declare no competing financial interest.

ACKNOWLEDGMENTS

This work was supported by JSPS KAKENHI Grant Numbers JP20H05840 (Grant-in-Aid for Transformative Research

Areas, "Dynamic Exciton"), JST, the establishment of university fellowships towards the creation of science technology innovation, Grant Numbers JPMJFS2123, JP17H01231, and JP17J09631. Computation time was provided by the Super Computer System, Institute for Chemical Research, Kyoto University. Nuclear magnetic resonance and mass spectrometry measurements were supported by the international Joint Usage/Research Center (iJURC) at the Institute for Chemical Research, Kyoto University. The authors thank Edanz Group (https://en-author-services.edanz.com/ac) for editing a draft of this manuscript.

REFERENCES

(1) Endo, A.; Ogasawara, M.; Takahashi, A.; Yokoyama, D.; Kato, Y.; Adachi, C. Thermally activated delayed fluorescence from Sn(4+)-porphyrin complexes and their application to organic light emitting diodes–a novel mechanism for electroluminescence. *Adv. Mater.* **2009**, *21*, 4802.

(2) Kaji, H.; Suzuki, H.; Fukushima, T.; Shizu, K.; Suzuki, K.; Kubo, S.; Komino, T.; Oiwa, H.; Suzuki, F.; Wakamiya, A.; et al. Purely organic electroluminescent material realizing 100% conversion from electricity to light. *Nat. Commun.* **2015**, *6*, No. 8476.

(3) Lin, T.-A.; Chatterjee, T.; Tsai, W.-L.; Lee, W.-K.; Wu, M.-J.; Jiao, M.; Pan, K.-C.; Yi, C.-L.; Chung, C.-L.; Wong, K.-T.; Wu, C. C. Sky-Blue Organic Light Emitting Diode with 37% External Quantum Efficiency Using Thermally Activated Delayed Fluorescence from Spiroacridine-Triazine Hybrid. *Adv. Mater.* **2016**, *28*, 6976.

(4) Uoyama, H.; Goushi, K.; Shizu, K.; Nomura, H.; Adachi, C. Highly efficient organic light-emitting diodes from delayed fluorescence. *Nature* **2012**, *492*, 234.

(5) Wong, M. Y.; Zysman-Colman, E. Purely Organic Thermally Activated Delayed Fluorescence Materials for Organic Light-Emitting Diodes. *Adv. Mater.* **2017**, *29*, No. 1605444.

(6) Godumala, M.; Choi, S.; Cho, M. J.; Choi, D. H. Recent breakthroughs in thermally activated delayed fluorescence organic light emitting diodes containing non-doped emitting layers. *J. Mater. Chem. C* **2019**, *7*, 2172.

(7) Yang, Z.; Mao, Z.; Xie, Z.; Zhang, Y.; Liu, S.; Zhao, J.; Xu, J.; Chi, Z.; Aldred, M. P. Recent advances in organic thermally activated delayed fluorescence materials. *Chem. Soc. Rev.* **2017**, *46*, 915.

(8) Im, Y.; Kim, M.; Cho, Y. J.; Seo, J.-A.; Yook, K. S.; Lee, J. Y. Molecular Design Strategy of Organic Thermally Activated Delayed Fluorescence Emitters. *Chem. Mater.* **2017**, *29*, 1946.

(9) Chen, W.-C.; Zhu, Z.-L.; Lee, C.-S. Organic Light-Emitting Diodes Based on Imidazole Semiconductors. *Adv. Opt. Mater.* **2018**, *6*, No. 1800258.

(10) Huang, Z.; Xiang, S.; Zhang, Q.; Lv, X.; Ye, S.; Guo, R.; Wang, L. Highly efficient green organic light emitting diodes with phenanthroimidazole-based thermally activated delayed fluorescence emitters. *J. Mater. Chem. C* **2018**, *6*, 2379.

(11) Lee, J.; Shizu, K.; Tanaka, H.; Nakanotani, H.; Yasuda, T.; Kaji, H.; Adachi, C. Controlled emission colors and singlet−triplet energy gaps of dihydrophenazine-based thermally activated delayed fluorescence emitters. *J. Mater. Chem. C* **2015**, *3*, 2175.

(12) Hall, D.; Rajamalli, P.; Duda, E.; Suresh, S. M.; Rodella, F.; Bagnich, S.; Carpenter-Warren, C. L.; Cordes, D. B.; Slawin, A. M. Z.; Strohriegl, P.; et al. Substitution Effects on a New Pyridylbenzimidazole Acceptor for Thermally Activated Delayed Fluorescence and Their Use in Organic Light-Emitting Diodes. *Adv. Opt. Mater.* **2021**, *9*, No. 2100846.

(13) Ohsawa, T.; Sasabe, H.; Watanabe, T.; Nakao, K.; Komatsu, R.; Hayashi, Y.; Hayasaka, Y.; Kido, J. A Series of Imidazo[1,2-f]phenanthridine-Based Sky-Blue TADF Emitters Realizing EQE of over 20%. *Adv. Opt. Mater.* **2019**, *7*, No. 1801282.

(14) Yi, R.-H.; Liu, G.-Y.; Luo, Y.-T.; Wang, W.-Y.; Tsai, H.-Y.; Lin, C.-H.; Shen, H.-L.; Chang, C.-H.; Lu, C.-W. Dicyano-Imidazole: A Facile Generation of Pure Blue TADF Materials for OLEDs. *Chem.-Eur. J.* **2021**, *27*, 12998.

(15) Frisch, M. J.; Trucks, G. W.; Schlegel, H. B.; Scuseria, G. E.; Robb, M. A.; Cheeseman, J. R.; Scalmani, G. B.V.; Petersson, G. A.; Nakatsuji, H.; Li, X.. et al.*Gaussian 16*. Rev. C.01. Gaussian, Inc.: Wallingford CT, 2016.

(16) TURBOMOLE V7.4.1 2019. *A Development of University of Karlsruhe and Forschungszentrum Karlsruhe GmbH, 1989-2007*. TURBOMOLE GmbH: http://www.turbomole.com, 2010.

(17) Hättig, C.; Weigend, F. CC2 excitation energy calculations on large molecules using the resolution of the identity approximation. *J. Chem. Phys.* **2000**, *113*, 5154.

(18) Han, C.; Zhao, Y.; Xu, H.; Chen, J.; Deng, Z.; Ma, D.; Li, Q.; Yan, P. A Simple Phosphine−Oxide Host with a Multi-insulating Structure: High Triplet Energy Level for Efficient Blue Electrophosphorescence. *Chem.-Eur. J.* **2011**, *17*, 5800.

(19) Tsai, M.-H.; Lin, H.-W.; Su, H.-C.; Ke, T.-H.; Wu, C.-C.; Fang, F.-C.; Liao, Y.-L.; Wong, K.-T.; Wu, C.-I. Highly Efficient Organic Blue Electrophosphorescent Devices Based on 3,6-Bis(triphenylsilyl)-carbazole as the Host Material. *Adv. Mater.* **2006**, *18*, 1216.

(20) Cai, X.; Su, S.-J. Marching Toward Highly Efficient, Pure-Blue, and Stable Thermally Activated Delayed Fluorescent Organic Light-Emitting Diodes. *Adv. Funct. Mater.* **2018**, *28*, No. 1802558.

(21) Goushi, K.; Yoshida, K.; Sato, K.; Adachi, C. Organic light-emitting diodes employing efficient reverse intersystem crossing for triplet-to-singlet state conversion. *Nat. Photon.* **2012**, *6*, 253.

(22) Duan, L.; Hou, L.; Lee, T.-W.; Qiao, J.; Zhang, D.; Dong, G.; Wang, L.; Qiu, Y. Solution processable small molecules for organic light-emitting diodes. *J. Mater. Chem.* **2010**, *20*, No. 6392.

(23) Zhang, S.; Ye, L.; Zhang, H.; Hou, J. Green-solvent-processable organic solar cells. *Mater. Today* **2016**, *19*, 533.

(24) Zheng, L.; Xu, J.; Feng, Y.; Shan, H.; Fang, G.; Xu, Z.-X. Green solvent processed tetramethyl-substituted aluminum phthalocyanine thin films as anode buffer layers in organic light-emitting diodes. *J. Mater. Chem. C* **2018**, *6*, 11471.

https://doi.org/10.1021/acsomega.2c01308
ACS Omega 2022, 7, 16740−16745